C 344.13 + C 344.1и
A - 99
3/XII-66
N.I.& M., 1967, v.51, N2, p. 309-314

ОБЪЕДИНЕННЫЙ
ИНСТИТУТ
ЯДЕРНЫХ
ИССЛЕДОВАНИЙ
Дубна

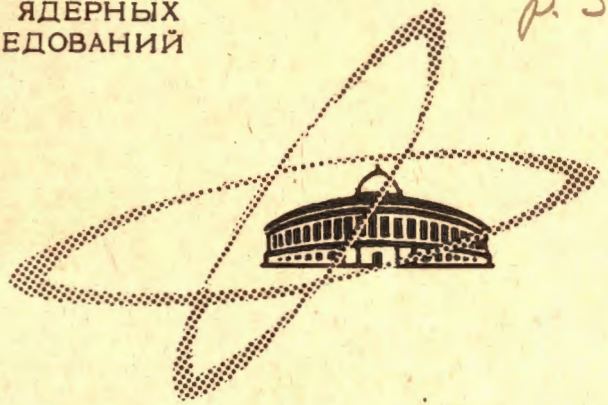

E13 - 2971

M.A. Azimov, A.S. Belousow , I.V. Chuvilo,
R. Firkowski, M.N. Khachaturyan, M.S. Khvastunov,
L.G. Makarov, E.I. Maltsev, A.T. Matyushin,
V.T. Matyushin, V.S. Pantuyev, L.N. Shtarkov ,
D.V. Uralsky, B.A. Zelenov, L.I. Zhuravleva

NEW METHOD FOR MEASURING THE EFFECTIVE MASS IN THE DECAYS: $x \to \gamma + \gamma$

1966

ЛАБОРАТОРИЯ ВЫСОКИХ ЭНЕРГИЙ

E13 - 2971

4617/1 p8.

M.A. Azimov, A.S. Belousow*, I.V. Chuvilo,
R. Firkowski, M.N. Khachaturyan, M.S. Khvastunov,
L.G. Makarov, E.I. Maltsev, A.T. Matyushin,
V.T. Matyushin, V.S. Pantuyev, L.N. Shtarkov*,
D.V. Uralsky, B.A. Zelenov, L.I. Zhuravleva

NEW METHOD FOR MEASURING THE EFFECTIVE MASS IN THE DECAYS: $x \to \gamma + \gamma$

* The Lebedev Physical Institute of the USSR Academy of Sciences
Moscow

Объединенный институт ядерных исследований БИБЛИОТЕКА

1. Introduction

One of the basic branches of elementary particle physics in recent years has been the discovery and systematization of resonances (resonance quantum numbers, decay modes and other characteristics). The study of resonance radiative decays is of special interest in view of the check of various symmetry theories, (-parity conservation In electromagnetic interactions and other problems. However, the present day methods for studying radiative decays have some disadvantages. Such effective methods, as for instance bubble and spark chambers allow to measure only one parameter, namely, an angle between particle decay products. Energy characteristics are either not measured or measured rather approximately. Naturally, such information does not permit to explicitely analyse each event and requires rich statistics. All these disadvantages are especially noticeable when a study is made of very rare events for whose identification the knwoledge of some basic parameters of the process under study is necessary.

In 1964 a new method[1,2,3] was proposed at the Laboratory of High Energies in Dubna to study resonance radiative decays which permits to directly measure particle effective mass in the decays:

$$\begin{matrix} \gamma + \gamma \\ e^+ + e^- \\ \pi^0 + \gamma \\ \pi^0 + \pi^0 \end{matrix} \qquad \text{etc.} \qquad (1)$$

The effective mass for decays (1) can be determined by means of the formula:

$$M^2 = (\Sigma E_i)^2 - (\Sigma \vec{p}_i)^2 \ . \qquad (2)$$

In the case of two-particle reactions for the first two of the above decays formula (2) is written as:

$$M^2 = 2E_1E_2(1-\cos\theta) . \qquad (3)$$

From formula (3) it is seen that in order to determine the square of the effective mass M^2 it is nesessary to measure three parameters: the energies E_1 and E_2 of the resonance decay products and the angle of opening θ between them (all the values are given in the lab. system).

Our method for effective mass measurements implies the use of the two-channel system of jointly operating spark chambers to determine the angle θ between resonance decay products and total absorption Gerenkov gamma-spectrometers to determine the particle energies E_1 and E_2. The kinematic analysis of reaction (1) shows that the geometry is optimal when the direction of gamma-quanta emission at a minimum angle coincides with the axes of detectors. In the above geometry the setup selects interactions when the momentum transferred to the nucleon is small. The optimum geometry and efficiency curves versus the momentum transfer were calculated by means of the electronic computer. The analysis of the energy spectra of gamma-quanta from decay (1) in the optimum geometry shows that within solid angles viewed by detectors the energy spectra of gamma-quanta (electrons, etc.) have their peak in each channel at $E_1=E_2=E/2$, where E is the incident particle energy. It is easy to show that another condition also holds, namely: the sum of energies E_1+E_2 (within the accuracy of the momentum transferred to the nucleon) is E. The above relations obtained from process kineamtics alow to introduce a logic system for selecting events, which in turn makes it possible to reduce the background.

2. Experimental Arrangement

The schematic view of the setup is shown in fig. 1. The scintillation counters S_1 and S_2 having dimensions 7 x 7 cm^2 are used for monitoring the incident particle beam. The spark chambers Sch_1 and Sch_2 in each of the two similar channel are a system of four modules having the dimensions of the active area 50 x 50 cm^2. In order to effectively detect tracks to a given accuracy the spark gap was taken to be 10 cm. Chamber side walls are made of glass. Electrodes are duralumin plates 60 x 60 cm^2 large and 1 mm thick forced with a frame 5 mm thick of the same material. The chambers are filled with neon-helium mixture. The overall volume of the chambers is 200 litres. The frames of reference and the tracks are photographed in two orthogonal projections per picture of the 35 mm film with a photodetector operating in the pulse regime from a triggering programme system.

A high voltage pulse per pair of symmetrically connected spark chambers is produced by two Arkadiev-Marx generators. When a generator is loaded with two cables a pulse amplitude on the chamber electrodes amounts to about 150 kv, the pulse front being about 2.10^{-8} sec, pulse duration being about 6.10^{-8} sec (at a 50% level). The first of the four spark chamber modules (with respect to the beam) in each channel are anticoincidence ones. In order to identify particles of the shower origin brass convertors about 0,4 rad. length thick are placed in front of the second and subsequent chambers. The scintillation counters S_3 and S_4 50×50 cm^2 large are placed between spark chambers and Cerenkov gamma-spectrometers in order to increase the efficiency of triggering the system by means of shower particles. Special lead glass of high transparency and with dimensions $50 \times 50 \times 30$ cm^3 and $50 \times 50 \times 20$ cm^3, respectively, is used as radiator material in Cerenkov gamma-spectrometers. Cerenkov radiation is collected by means of nine photomultipliers having a 17 cm photocathode diameter. The photomultipliers are fixed at one of the radiator sides. Reflectors of aluminum foil are fastened at the remaining sides of the radiator. The block-diagramm of the electronics is shown in fig. 2. A spark chamber system is triggered by the $S_1\ S_2\ S_3\ S_4\ C_1\ C_2$ pulse under the condition that:

1. The energies E_1 and E_2 of particle decay products exceed some threshold energy E_{ki}: $E_1 \geq E_{ki}$, $E_2 \geq E_{ki}$.

2. The sum of the energies E_1 and E_2 satisfies the condition $E_1 + E_2 \geq E_n$.

The threshold values of E_{ki} and E_n are taken basing on the process kinematic analysis and the energy resolution of gamma-spectrometers. Pulses from Cerenkov gamma-spectrometers are selected with discriminators. The sum energy threshold is established by the third discriminator connected after a circuit summing pulses from two spectrometers. The discriminators exclude the delay spread of output signals with respect to the amplitude and the shape of input pulses. Spectrometer channels consist of linear gates, amplitude analysers and detectors. The analysers are a combination of amplitude coders with scalers. The counts of scalers are detected with a printer and also (pulse amplitudes from the first and second gamma-spectrometers) are photographed in the proper picture. Thus, all event information θ, E_1, E_2 (angles and energies) is present in the film.

3. Calibration

Cerenkov gamma-spectrometers were calibrated by electrons in the energy range from 1 to 4 GeV[3]. As is seen from fig. 3, calibration curves for both the spectrometers are linear up to 4 GeV within experimental errors. The energy

resolutions of the spectrometers in the above energy range is weakly dependent on energy and is about $\pm$ 5-7%. (See fig. 4). To improve the values of E_1 and E_2 obtained experimentally and to introduce for each event the corresponding corrections taking into account the angle and the plase of gamma-quanta entering the radiator of the Cerenkov counter, gamma-spectrometers were additionally calibrated with the electron beam over the whole surface and in the operating angle region.

Apparatus calibration over effective masses was made by means of the decays:

$$\eta^0 \to \gamma + \gamma \qquad (4)$$

η^0 -mesons were produced by 4.0 GeV/c negative pions in a polyethelene target. An effective mass was measured for 80 events that could be interpreted as the neutral particle decay into two gamma-quanta (4). The obtained effective mass and opening angle distributions for the above-mentioned events are shown in figs. 5 and 6. As is seen from fig. 5, the effective mass distribution exhibits a pronounced peak at M = 550 MeV which is due to the η^0 -meson decay into two gamma-quanta. A peak is also observed in the angular distribution of gamma-gamma events at an angle equal to the minimum one for decays (4) at 4 GeV. For an additional analysis of data and for η -meson event separation from the background each event is shown in fig. 7 as a point at a plane where two gamma-quanta energy ratio E_1/E_2 is given at the ordinate whereas the angle of opening between them θ is presented at the abscissa. The solid curve (2) is a theoretical one correlating the energy ratio and the opening angle for 4 GeV η^0 -mesons. The dashed curves (1 and 3) show apparatus and angle resolution. As is seen from fig. 7, 49 from 80 events are in the corridor of errors equal to two standard deviations. These events can be indentified as the $\eta^0 \to 2\gamma$ decays. The effective mass and opening angle distributions for the above-mentioned events are shown in figs. 8 and 8a. As is seen from the figs., the curves are only slightly changed after selection. Indeed, the number of events in the effective mass distribution peak and the number of events having an angle close to minimal in the opening angle distribution remains constant. The obtained experimental data allow to calculate the η^0 -meson production crosssection in the reaction $\pi^- + p \to n + \eta^0$ at 4GeV. In the calculations use was made of the efficiency curves for the apparatus which had been obtained by the Monte-Carlo method using the electronic computer(fig. 9 and 10). Taking into account the relative probability for the $\eta^0 \to \gamma + \gamma$ decay (38,6%) for the η^0 -meson production cross section the value of (74$\pm$12) mb was obtained which is in good agreement with the data of other authors.

Conclusion

The suggested method for investigating resonance radiative decays by means of a two-channel system of jointly operating spark chambers and Cerenkov gamma-spectrometers permits:

1. To simultaneously measure some processes having similar kinematics and identical logics.

2. To analyse each event separately.

3. To measure the angles and energies of resonance decay products and hence, to obtain the effective mass.

4. To introduce the proper logics for selesting events which takes into account the kinematics of the process under study and thus to considerably reduce the background triggering.

5. To carry out experiments in conditions of large loads (10^5 and more particles per burst).

References

1. M.A. Azimov, A.M. Baldin, V.S. Pantuyev, M.N. Khachaturyan, I.V. Chuvilo. Internal Report B-7-2070, Dubna, 1964.
2. M.A. Azimov, V.S. Pantuyev, M.N. Khachaturyan, I.V. Chuvilo. Preprint-173 Dubna, 1964.
3. M.N. Khachaturyan, M.A. Azimov, V.S. Pantuyev. Priority certificate No. 182249.

Received by Publishing Department
on September 12, 1966

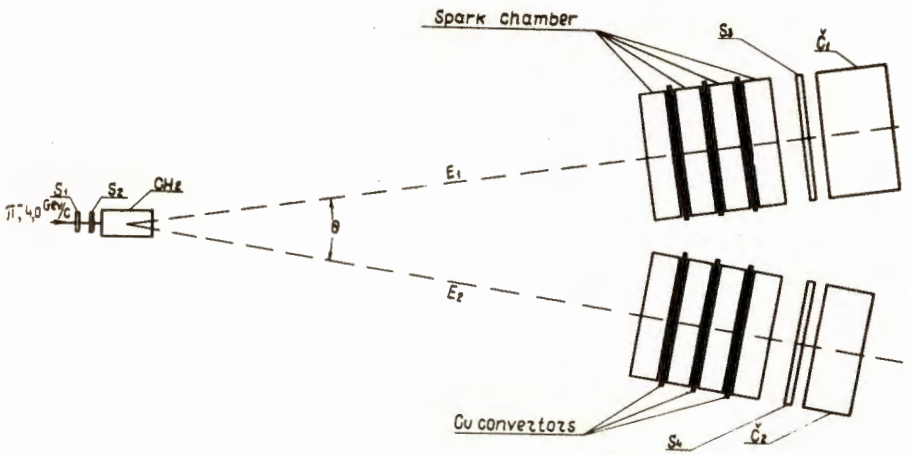

Fig. 1. Schematic view of the apparatus.
$S_1 \ldots S_4$ - scintillation counters.
C_1, C_2 - Cerenkov total absorption gamma-spectrometers.
Cu - brass convertors, each 6 mm thick.
CH_2 - a polyethelene target.

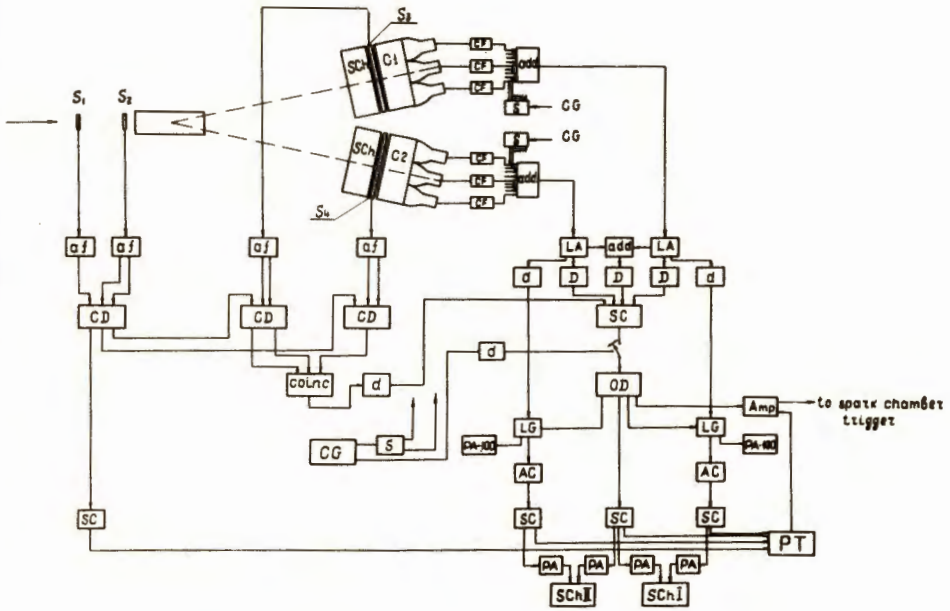

Fig. 2. Block diagram of the electronics.
af - amplifier-shaper, cd - coincidence and discriminator circuit, sc - scaler, coinc. - coincidence circuit, d - delay circuit, cg - control generator, s - splitter, D - discriminator, LA - linear amplifier, add - adding circuit, SC - slow coincidence circuit, OD - output discriminator, LG - linear gate, AC - amplitude convertor, P - printer, CF - cathode follower, Amp - amplifier, PA - power amplifier, PA-100 - a hundred-channel pulse-height analyser, $S_1 \ldots S_4$ - scintillation counters, C_1, C_2 - Cerenkov gamma-spectrometers, SCH - spark chambers.

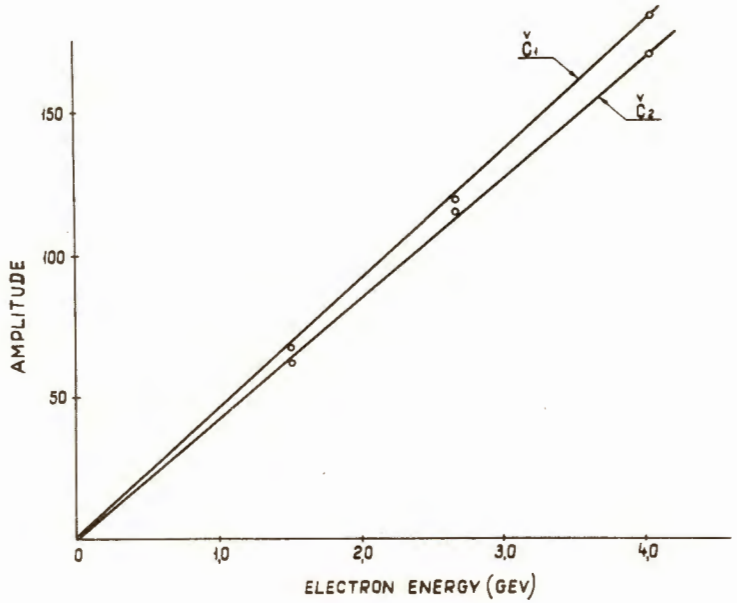

Fig. 3. Calibration curves for the 1-st and 2-nd Cerenkov gamma-spectrometers obtained with 1.5 GeV, 2.5 GeV and 4.0 GeV electron beams.

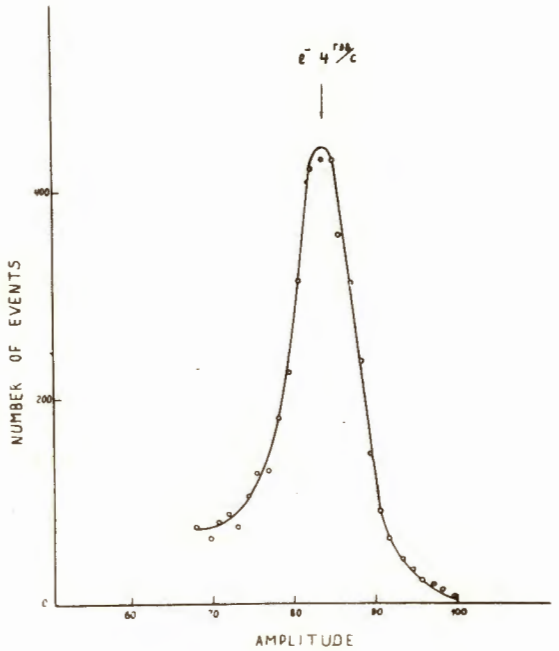

Fig. 4. Amplitude distribution of pulses from one of the Cerenkov gamma-spectrometer obtained with a 4 GeV electron beam.

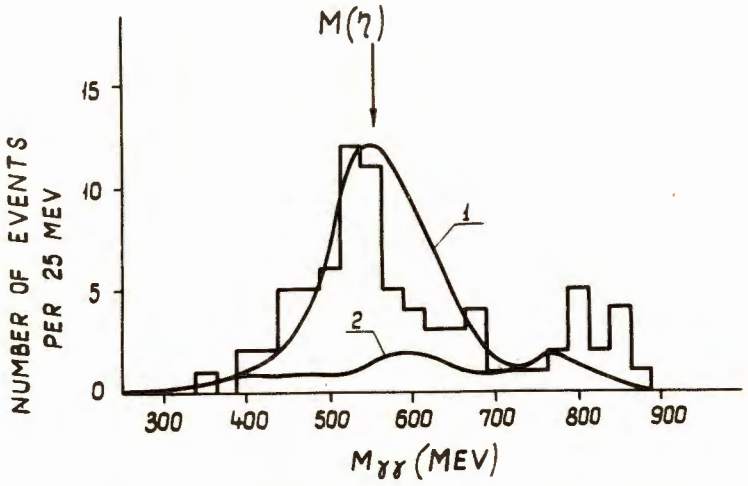

Fig. 5. Effective mass distributions obtained experimentally for 80 decays: $\chi^0 \to \gamma + \gamma$. Curve (1) has been obtained by the Monte-Carlo method by modelling the processes:

$$\pi^- + p \to \begin{cases} N + \eta^0 & (\eta^0 \to \gamma + \gamma) \\ N + \pi^0 + \pi^0 & \\ N + \pi^0 + \eta^0 & \\ N + \omega^0 & (\omega^0 \to \pi^0 + \gamma) \\ N + f^0 & (f^0 \to \pi^0 + \pi^0) \end{cases}$$

using the electronic computer. Curve (2) is a background curve (the sum of processes 2-5).

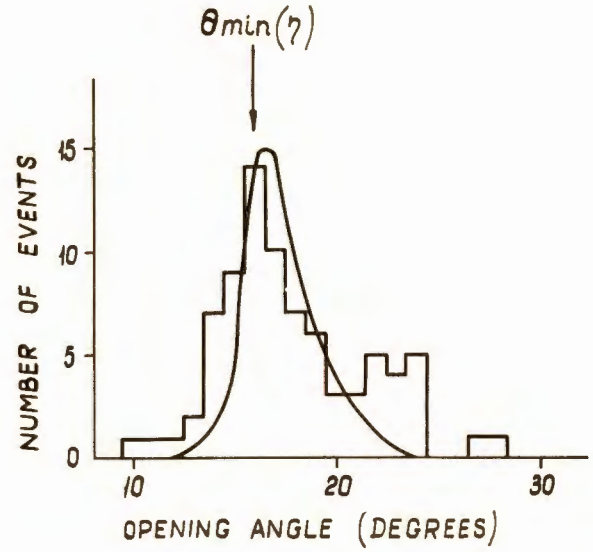

Fig. 6. Experimental opening angle distributions for 80 events. Solid line is a Monte-Carlo generated curve for the process $\pi^- + p \to n + \eta^0 (\eta^0 \to \gamma\gamma)$.

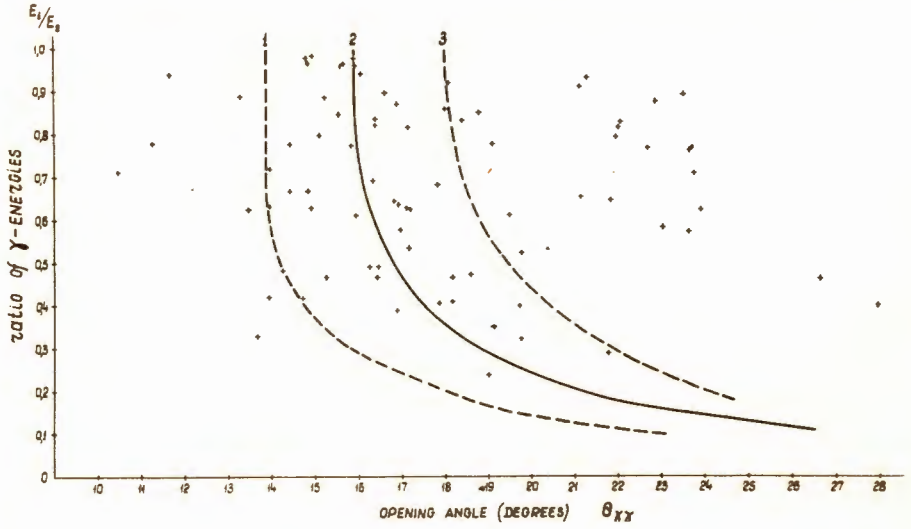

Fig. 7. Correlation between the energy ratio of the two showers of each events and the angle of opening. The solid line gives theoretically expected correlation for η^0 's at 4.0 GeV (2); the energy and angular resolution is indicated by two other (dashed) lines (1 and 3).

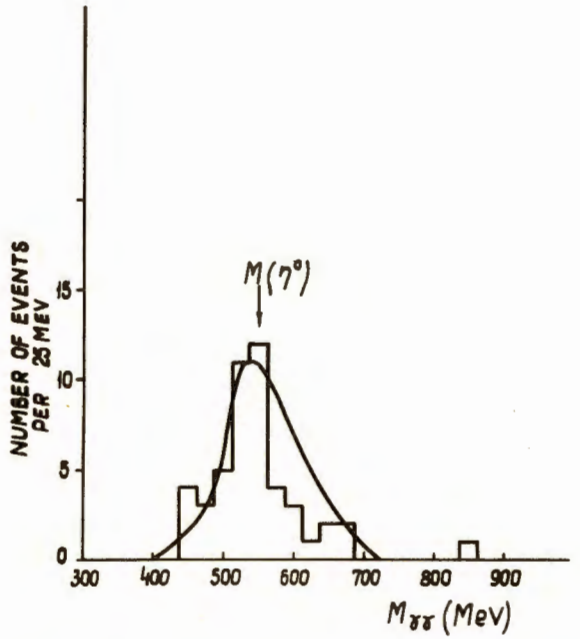

Fig. 8. Effective mass and opening angle distributions for 49 events selected by the kinematic analysis of the process $\pi^- + p \to n + \eta^0 (\eta^0 \to \gamma + \gamma)$ at P = 4.0 GeV/c.

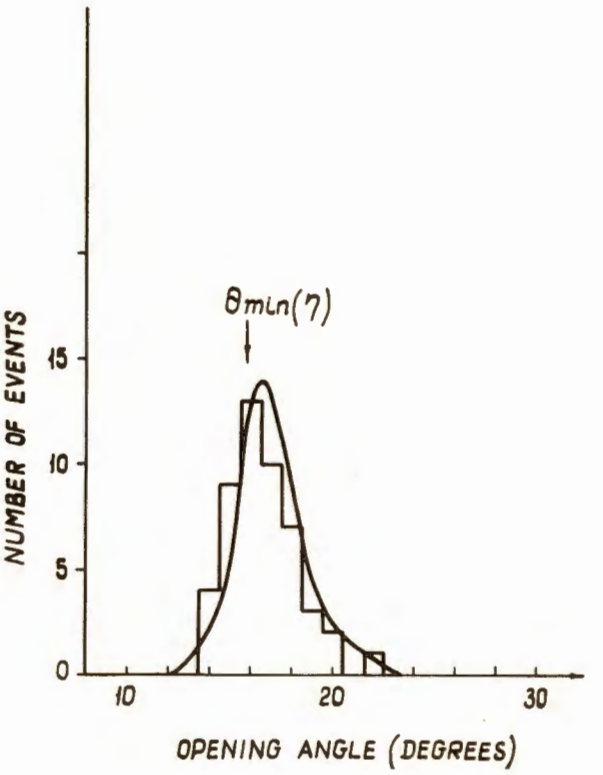

Fig. 8a.

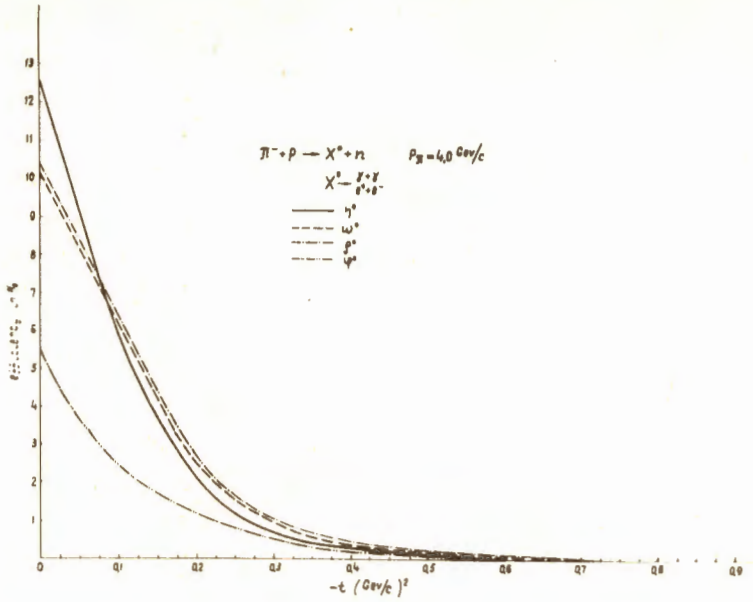

Fig. 9. Theoretical curves of resonance detection effeciency of the apparatus versus the four-momentum tramsfer calculated for the operating geometry (the angle between detector axes is 19°).

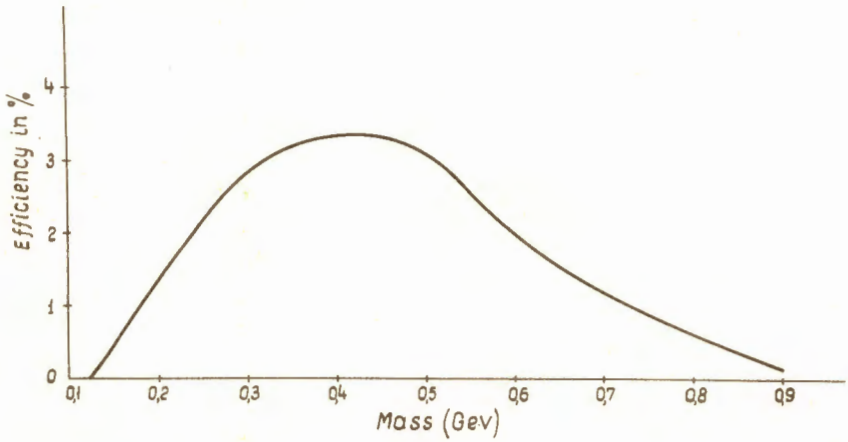

Fig. 10. Apparatus efficiency curve integrated over all the four-momenta transfer versus the decaying particle mass for the operating geometry (19°).